Cooling liquid flow boiling heat transfer in an annular minigap with an enhanced wall

Magdalena Piasecka[1,*], *Tomasz* Musiał[2], *Artur* Piasecki[3]

[1,2] Faculty of Mechatronics and Mechanical Eng., Kielce University of Technology, Al. 1000-lecia P.P. 7, 25-314 Kielce, Poland
[3] Circle of Health Tourism, Dabrowa 2, 26-001 Maslow, Poland

Abstract. The paper focused on flow boiling heat transfer in an annular minigap. This gap of 1 mm width was created between the metal pipe with an enhanced surface contacting fluid and the external glass pipe positioned along the same axis. The heated element for the HFE-649 flowing in the minigap was a cartridge heater. Thermocouples were used to measure the temperature of the metal pipe in the contact surface with a fluid. The local values of the heat transfer coefficient for stationary state conditions were calculated using an one-dimensional method in which the multilayer cylindrical wall was assumed to be planar. The results were presented as a function of the heat transfer coefficient along the minigap length and as boiling curves, prepared for selected values of mass flow rate and five types of the enhanced heated surface and a smooth one. Observations indicated that the highest local values of heat transfer coefficient were obtained with using the enhanced surface produced by electromachining process (spark erosion) at the saturated boiling region. The boiling curves generated for two distances from the minigap inlet have similar plots without a drop in the temperature of the heated surface characteristic for nucleation hysteresis.

1 Introduction

Recently, a lot of papers have been published to address the issues of heat transfer in flow boiling in minichannels of different geometry. In [1-4] the annular minigap geometry of the test section was used in experiments and their results were described.

Analysis of flow boiling heat transfer in annular minigaps was presented in [1]. The heat transfer coefficient during flow boiling of n-hexane was calculated based on measurement using infrared thermography to determine the axial wall temperature in the minigap. It was observed that the heat transfer coefficient increased significantly in the subcooled boiling, and after reaching a maximum at the transition to the saturated flow boiling, it drops almost monotonically with increasing vapour quality.

In [2] and [3], the results of R-407C flow boiling heat transfer were discussed for the subcooled and saturated boiling region, respectively. The main aim was to analyze how the channel size affects the subcooled flow boiling heat transfer and two-phase structures. Results of experiments in the subcooled boiling region were discussed in [2] and for the saturated boiling region - in [3]. It was observed that: the heat transfer coefficient increased with a decrease in the minigap and decreased with an increase in the inlet liquid subcooling, raising the heat flux caused a significant increase in the heat transfer coefficients but the effects of the mass flux and pressure (saturated temperature) on the boiling heat transfer coefficient were slighter.

Impact of minigap size on R-407C flow boiling heat transfer and bubble characteristics were analyzed in [4]. A horizontal annular minigap of the width 1 and 2 mm was used in experiments. It was noticed that the subcooled flow boiling heat transfer coefficient increases with a reduction in the minigap size and decreases with an increase in the inlet liquid subcooling. The influence of the refrigerant mass flux and saturated temperature on the boiling heat transfer coefficient were slighter. The boiling curves indicated appearance of the temperature overshoot at the incipience of boiling.

Heat transfer results obtained from experiments conducted with several boiling liquids (distilled water and refrigerants HFE-7100 and HFE-7000) flowing in an annular minigap of 1 mm depth were analyzed by the authors in [5-8]. Rectangular cross-section of the minichannel was applied in experiments conducted in the Kielce University of Technology for twenty years. Recent results were presented in [9-13]. The use of enhanced surfaces produced in thermal processes is known to intensify the heat transfer process [14-17], also in pool boiling heat transfer [18-25]. Heat transfer in confined spaces as face seals were analyzed in [26-28].

This research interest is focused on HFE-649 boiling heat transfer in an annular minigap heated by an enhanced metal surface produced by several technological processes. The one-dimensional mathematical method was used for calculations of the heat transfer coefficient. In previous authors' papers also two-dimensional mathematical methods were applied for the heat transfer coefficient determination [5, 7].

*Corresponding author: tmpmj@tu.kielce.pl

2 Experiment

2.1 Experimental stand

The experimental stand consists of several systems/loops, Fig. 1:

- the test loop with a minigap in which the working fluid (HFE-649, 3M) circulates, this loop comprises a mass flow meter, a heat exchanger, a gear pump, a compensating tank, a filter and a deaerator;
- the data and image acquisition system consist of: a data acquisition station, a high speed camera, the lighting and a computer with special software,
- the power supply and control system with an autotransformer as a power source, a shunt, a voltmeter and an ammeter.

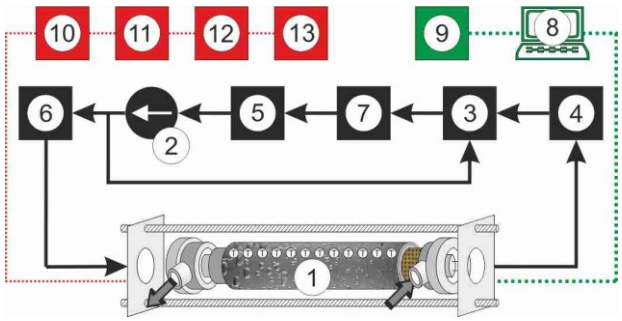

Fig. 1. The schematic diagram of a test section: 2- a gear pump, 3 - a compensating tank, 4 - a tube-type heat exchanger, 5 - a filter, 6 - a mass flow meter, 7 - a deaerator, 8 - a data acquisition station, 9 - a pc computer, 10 - an inverter welder, 11 - a voltmeter, 12 - an ammeter, 13 - a shunt.

The test section with an annular minigap is the essential element of the experimental stand, Fig. 2. The gap 1 mm wide (3) was created between a metal (copper) pipe (2) and a glass pipe (1) positioned along the same axis. Inside the metal pipe, a cartridge heater (4) was located axially and symmetrically, powered by autotransformer with adjusted current intensity. Thermocouples (6) were fixed with a spacing of 10 mm in the flow line and their wires run in the gap between the heater and the metal pipe in the thermal conductive filler layer. Two thermocouples and two pressure meters were installed at the inlet and outlet of the minigap in the test section headers (5).

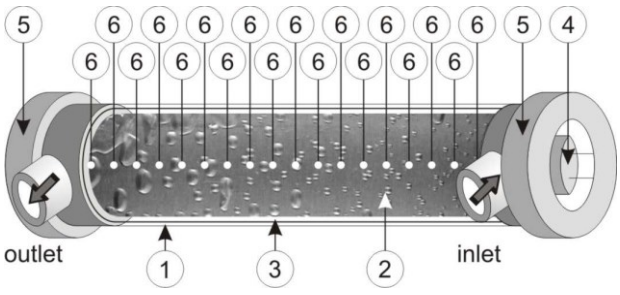

Fig. 2. The schematic diagram of the test section: 1- a glass pipe for viewing flow patterns, 2 - a copper pipe, 3 - an annular minigap, 4 - a cartridge heater, 5 - a test section header, 6 – a thermocouple.

Uncertainty of temperature measurement by thermocouples were estimated similarly as presented in [29].

Five enhanced surfaces of the metal pipe were used in experiments. These surfaces were produced by: sanding, electromachining process (spark erosion), threading (two types) and cutting. The 3D topographies of all enhanced surfaces contacting fluid in the minigap are presented in Fig. 3 Results from experiments when the smooth surface of the metal pipe were applied are also shown for comparison in Figs. 5-9.

2.2 Experimental methodology

During experimental series, after the deaeration, the working fluid (HFE-649) flows laminarly along the minigap. When flow rate and the pressure are fixed, there is a gradual increase in the electric power supplied to the heater followed by an increase in the heat flux transferred to the fluid in the minigap. This leads to the onset of nucleate boiling and the heat transfer enhancement. The flow structures on the outer surface of the metal pipe (smooth or enhanced) are monitored simultaneously.

3 Heat transfer coefficient determination

The heat transfer coefficient between the metal pipe surface and the HFE-649 flowing in a minigap was determined using the one-dimensional mathematical method presented in detail in [6]. It was assumed that the heat flow through the major elements of the test section is stationary and the elements create a system of planar layers with different thickness and thermal conductivity, Fig. 4. The thermal conductive filler layer was omitted (its thickness is in the order of 10^{-3} m). The dimension along the flow direction was denoted by z and perpendicular to the flow direction (related to the thickness of the heater) - by r. The local coefficients at the interface between the metal pipe surface and the fluid flowing in the minigap are determined from the following equation [6]:

$$\alpha(z_i) = \frac{0.5\, r_1\, q_V}{T_{s,i} - 0.5\, r_1\, q_V \dfrac{(r_3 - r_2)}{\lambda_M} - T_f(z)} \qquad (1)$$

where

q_V - volumetric heat flux, $q_V = I \cdot \Delta U / V_H$, I – current intensity, ΔU – voltage drop, V_H – volume of the heater;

$T_{s,i}$ – temperature measured by i-th thermocouple in a thermal conductive filler layer, it is assumed that it corresponds to temperature of the metal pipe;

T_f – fluid temperature, it is assumed that the fluid temperature varies linearly from the inlet fluid temperature $T_{f,in}$ to the outlet fluid temperature $T_{f,out}$ in the subcooled boiling region, while in the saturated boiling region the fluid temperature equals to the local saturation temperature calculated on the basis on pressure varying linearly from the inlet to the outlet.

The results from the saturated boiling region were omitted when the temperature difference was very small.

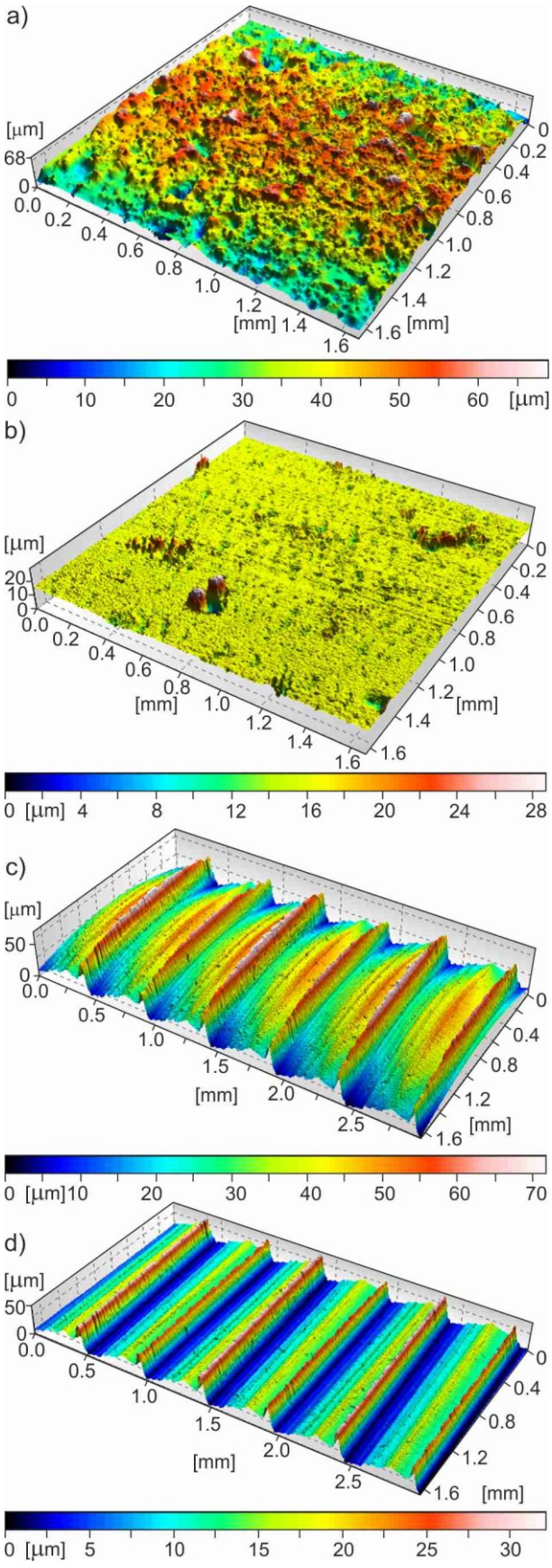

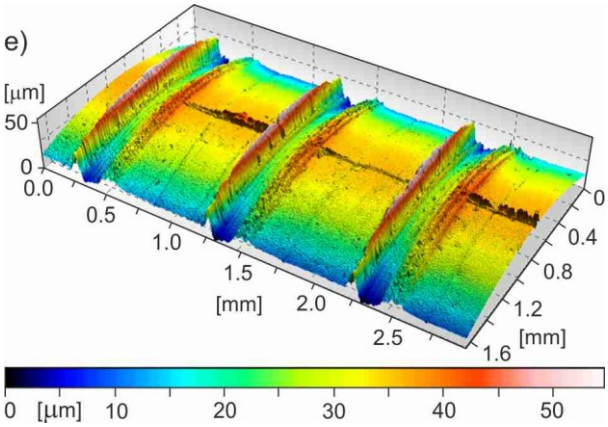

Fig. 3. 3D topographies of an enhanced metal surface contacting fluid in the minigap, produced by: a) sanding;
b) electromachining process, c,d) threading: type 1 (c) and type 2 (d); e) cutting.

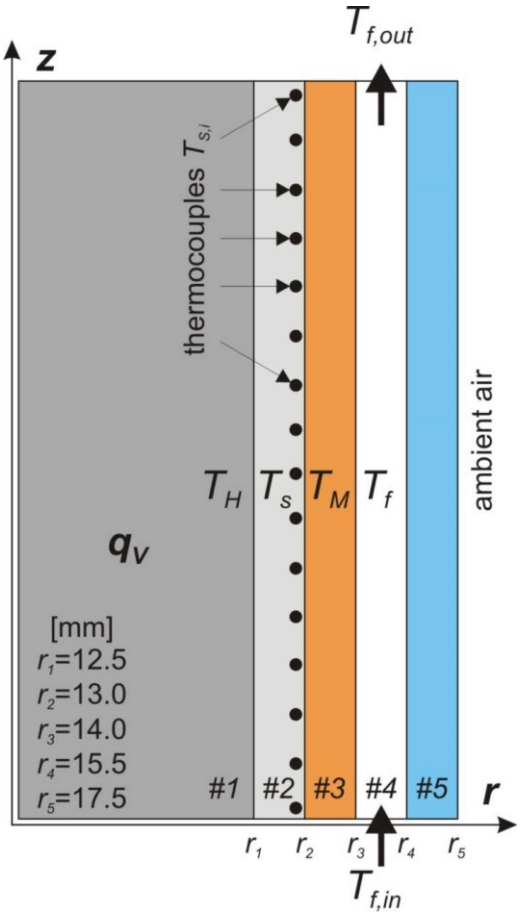

Fig. 4. A schematic diagram illustrating the assumptions adopted for the planar multilayer wall as horizontal cross-section, #1 - a cartridge heater, #2 - a thermal conductive filler layer, #3 - a metal pipe, #4 - a minigap, #5 - a glass pipe.

4 Results

The study shows the results obtained for the entire boiling region. The most important concern was to identify the heat transfer coefficient. The results from experiments were presented at the increasing heat flux being supplied to the heater versus the distance from the minigap inlet for selected values of mass flow rate.

Figures 5-9 refer to the five types of enhanced heated surfaces and a smooth one.

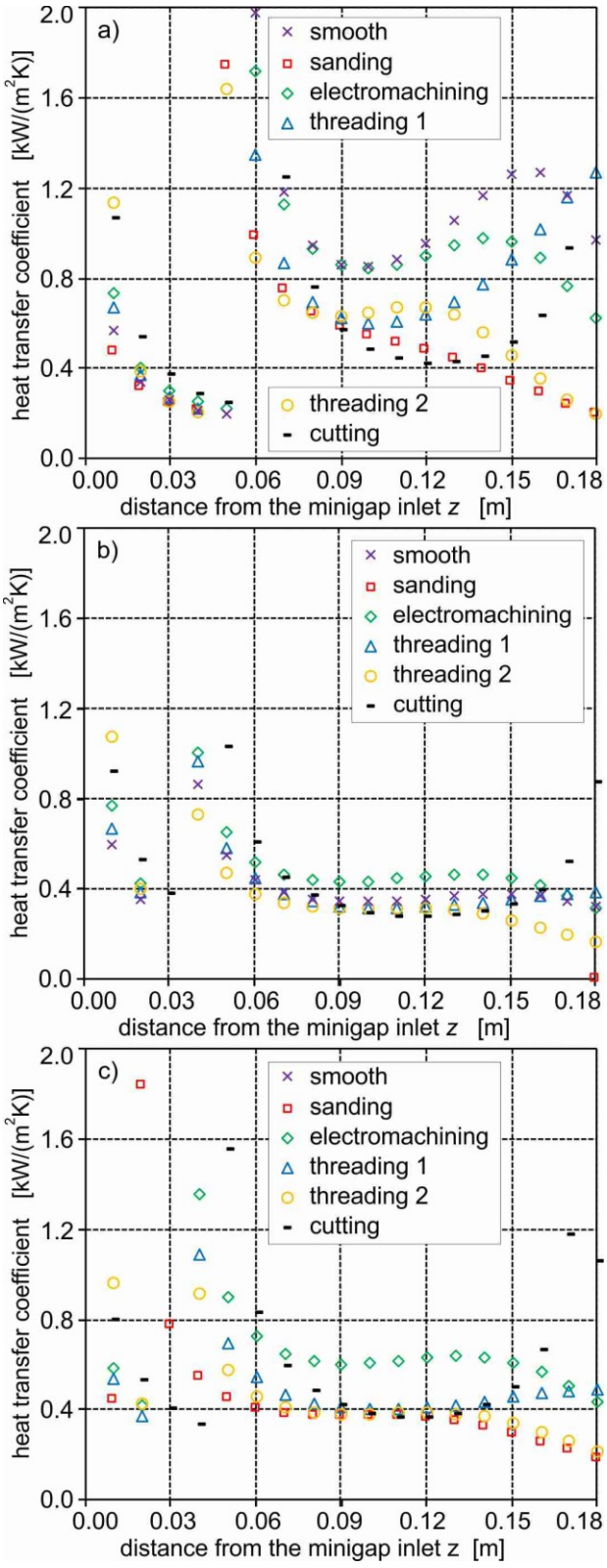

Fig. 5. Heat transfer coefficient vs. the minigap length, experimental parameters: mass flow rate of $2.22 \cdot 10^{-3}$ kg· s^{-1} a) q_w = 7 kW m^{-2}, b) q_w = 11 kW m^{-2} and c) q_w = 18 kW m^{-2}.

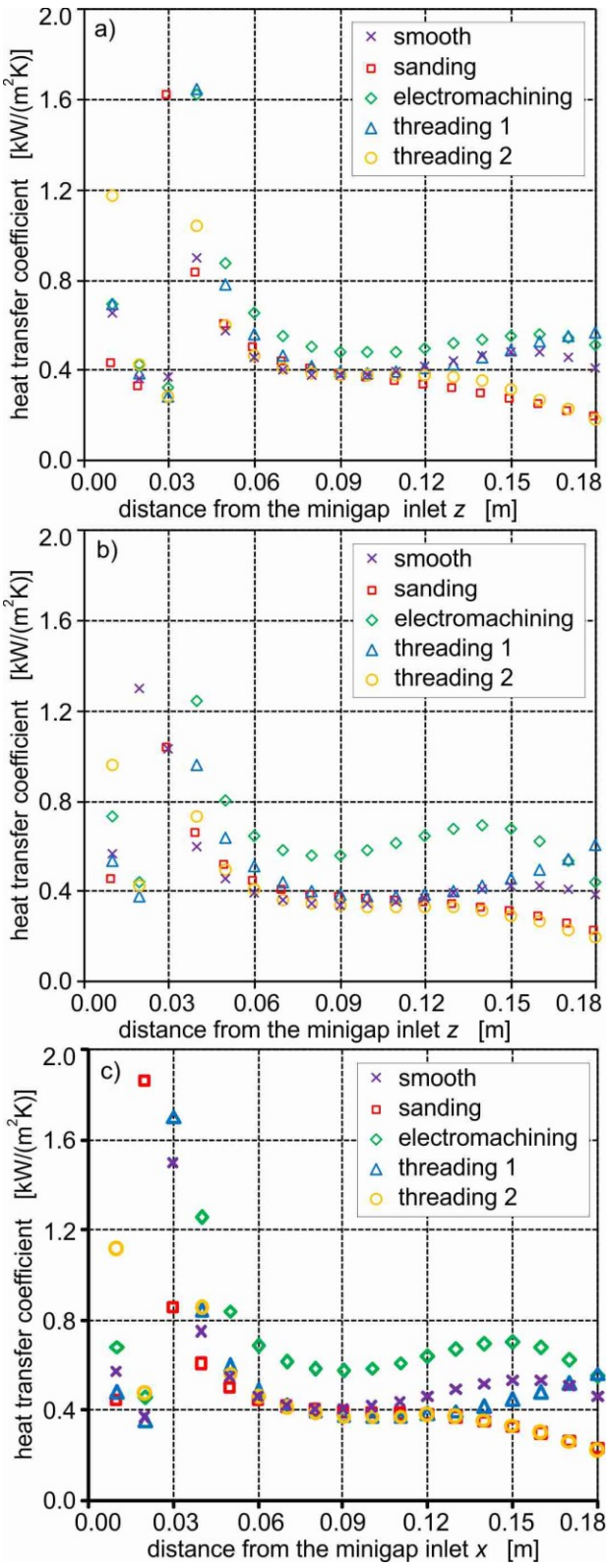

Fig. 6. Heat transfer coefficient vs. the minigap length, mass flow rate of $3.33 \cdot 10^{-3}$ kg·s^{-1}, a) q_w = 11 kW m^{-2}, b) q_w = 15 kW $m^{-2}$and c) q_w = 18 kW m^{-2}.

Experimental parameters for data presented in Figs. 6-9, are as follows:

- mass flow `rates: $2.22 \cdot 10^{-3}$ kg· s^{-1}, (Fig. 5), $3.33 \cdot 10^{-3}$ kg· s^{-1} (Fig. 6) and $6.67 \cdot 10^{-3}$ kg· s^{-1} (Fig. 7),
- values of heat flux: 7 kW m^{-2}, 11 kW m^{-2}, 15 kW m^{-2}, 18 kW m^{-2} or 24 kW m^{-2};
- inlet pressure in the range 150-350 kPa;
- inlet liquid subcooling in the range 40-70 K.

When analysing the results presented in Figs. 5-7 as the heat transfer coefficient vs. the distance from the minigap inlet, it can be noticed that the values of the coefficient were found to decrease with the minigap length in the subcooled boiling region. Under the saturated boiling, local heat transfer coefficients achieved higher values compared to those in the subcooled boiling region. When the saturated boiling region starts the values of the calculated heat coefficient are the highest and then they usually decrease with the distance from the gap inlet.

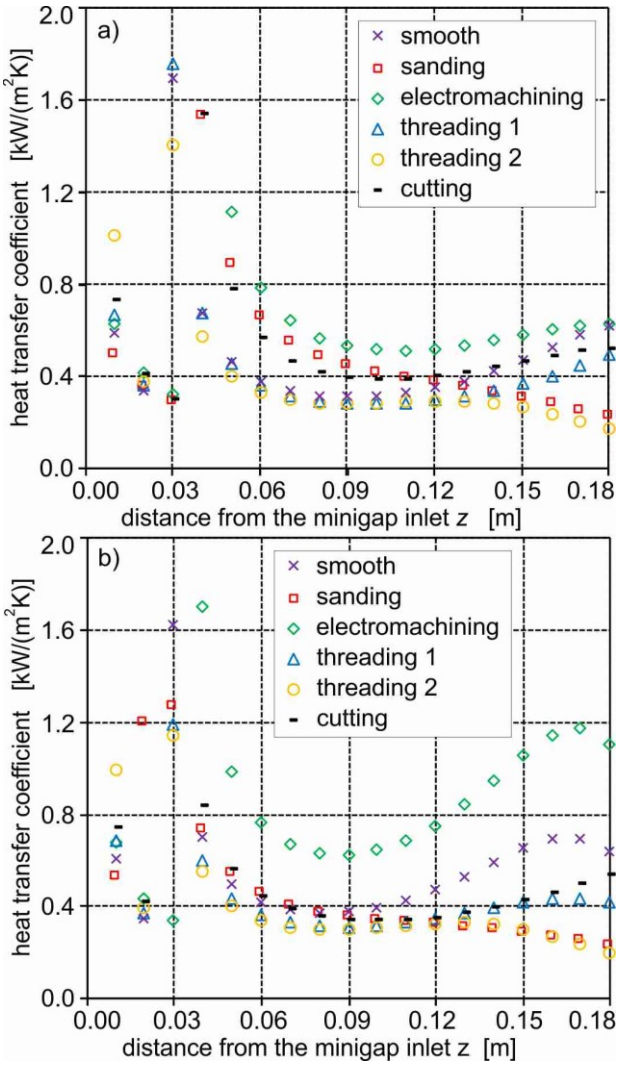

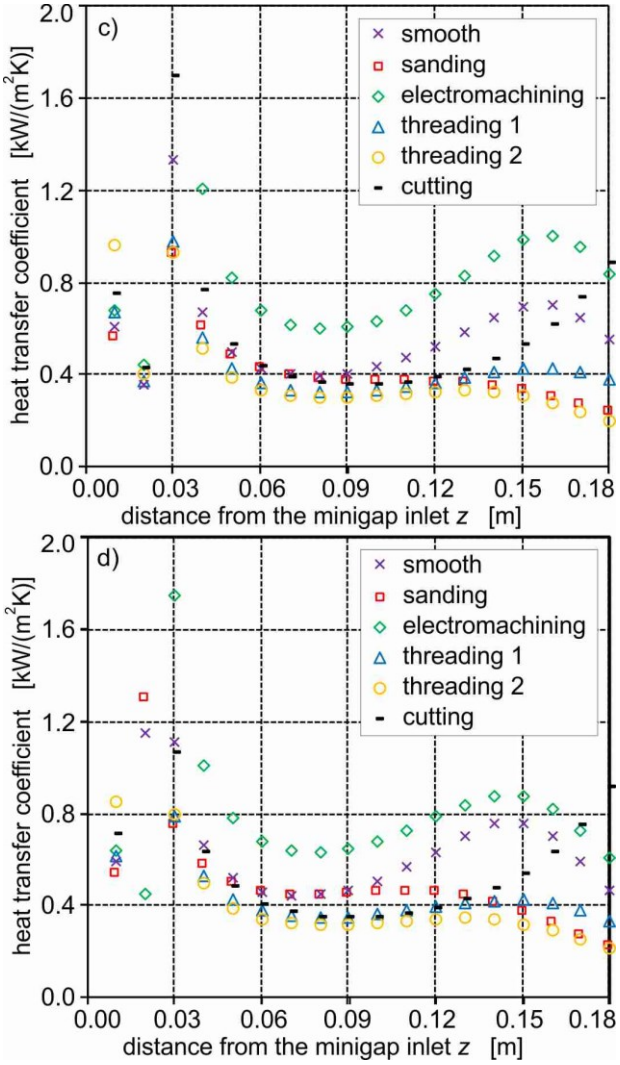

Fig. 7. Heat transfer coefficient vs. the minigap length, mass flow rate of $6.67 \cdot 10^{-3}$ kg·s^{-1}, a) q_w = 11 kW/m^2, b) q_w = 15 kW/m^2, c) q_w = 18 kW/m^2 and d) q_w = 24 kW/m^2.

The highest local values of heat transfer coefficient were obtained with using the enhanced surface produced by electromachining process (spark erosion) at the saturated boiling region - in comparison to other case and for all mass flow rates. The erosion process on the modified surface always leads to unevenly distributed minicavities [30,31]. Characteristics of enhanced heated surface obtained by spark erosion indicates that the layer of melted metal of the foil and an electrode material, a few μm high, accumulates around the cavities. Local values of heat transfer coefficient received for type 2 threaded surface (denoted as "threading 2") were the lowest, even compared with data obtained for a smooth surface. Probably this enhanced surface caused local inconvenience o create nucleation sites during fluid flow.

According to the results shown in Fig. 5a the heat transfer coefficient was the highest, not only at the beginning of the saturated boiling region for the lowest mass flow rate and the lowest analyzed heat flux at the developed nucleate boiling.

The boiling curves shown in Figs. 8 and 9 were plotted as the heat flux against the difference between temperature of the metal pipe T_M-and fluid temperature T_f , for 0.06 m and 0.12 m distances from the gap inlet.

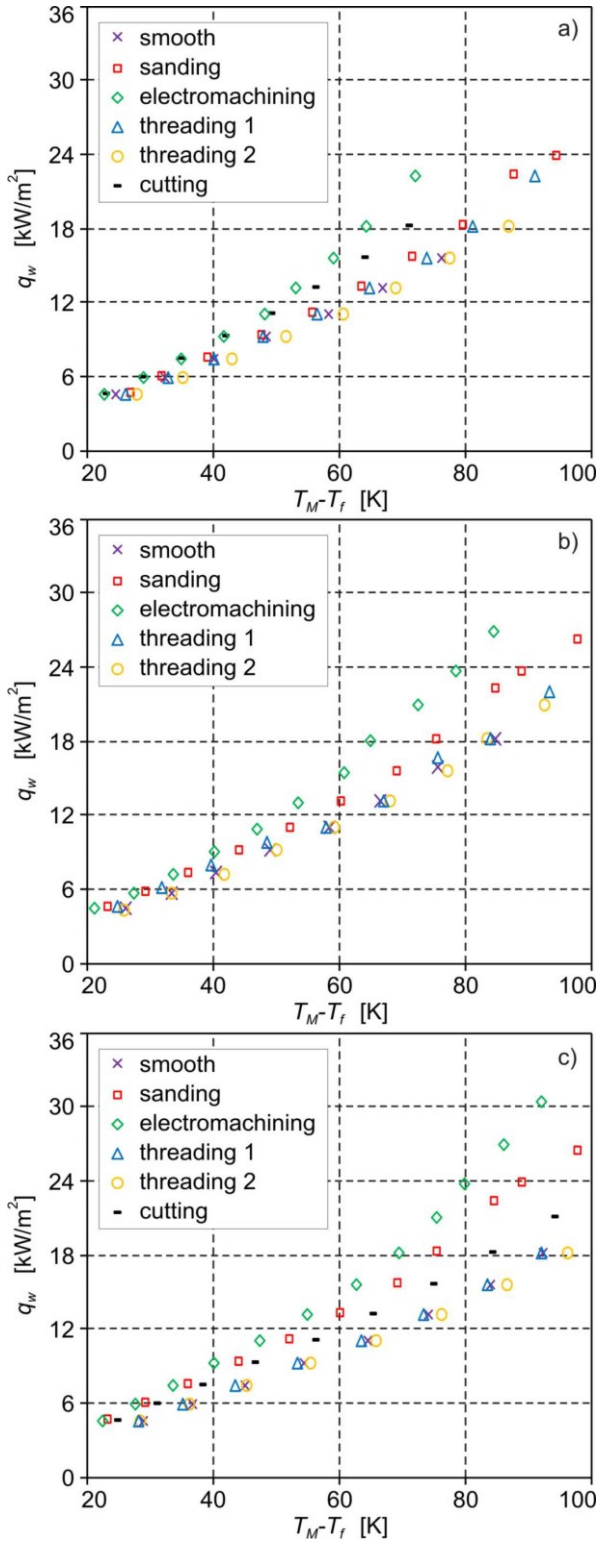

Fig. 8. Boiling curves generated for 0.06 m distance from the minigap inlet, constructed for all tested surfaces, T_M – temperature of the metal pipe, T_f – fluid temperature; at the following values of mass flow rate: a) 2.22· 10^{-3} kg· s^{-1}, b) 3.33· 10^{-3} kg· s^{-1} and c) 6.67· 10^{-3} kg· s^{-1}.

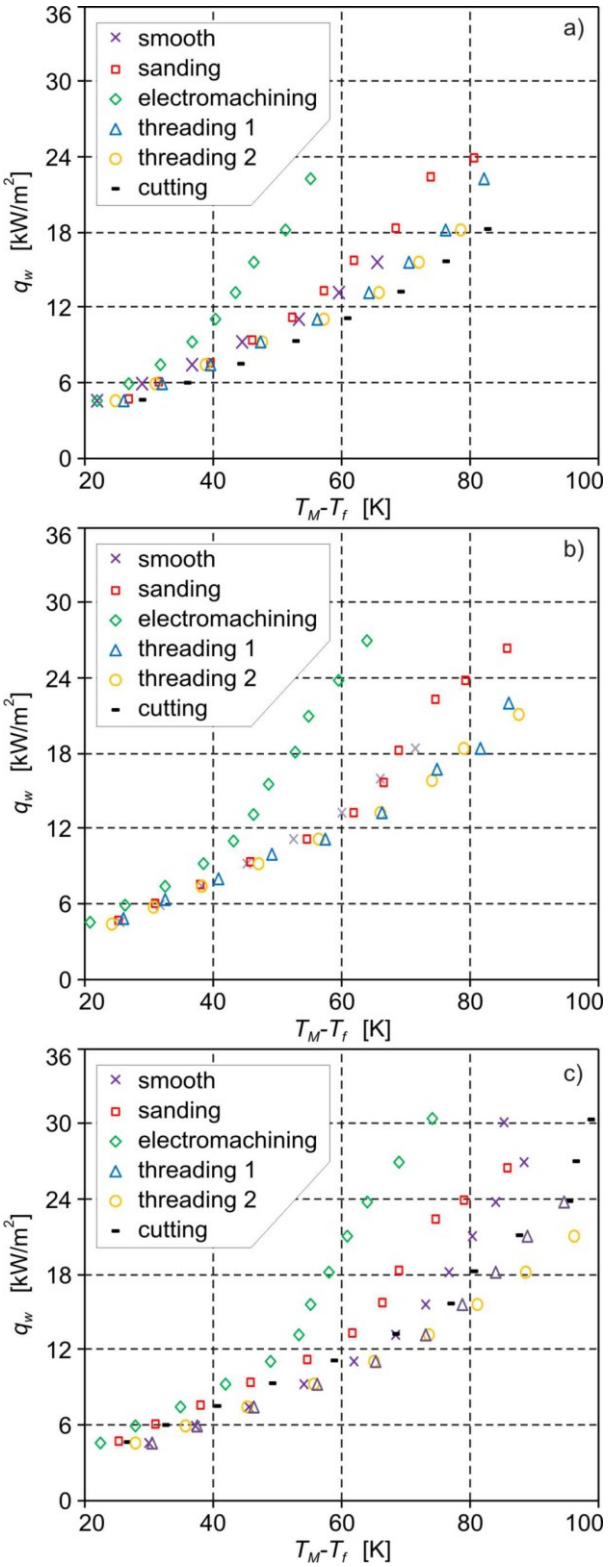

Fig. 9. Boiling curves generated for 0.12 m distance from the minigap inlet, constructed for all tested surfaces, T_M – temperature of the metal pipe, T_f – fluid temperature; at the following values of mass flow rate: a) 2.22· 10^{-3} kg· s^{-1}, b) 3.33· 10^{-3} kg· s^{-1} and c) 6.67· 10^{-3} kg· s^{-1}.

The boiling curves generated for 0.06 m distance from the inlet have similar plots. Similar values of the temperature difference T_M-T_f were observed for all mass velocities. Spontaneous nucleation at boiling incipience do not caused a drop in the temperature of the heated surface and the phenomenon known as "nucleation hysteresis".

The boiling curves prepared for 0.12 m distance from the inlet have rather similar course of plots. When analyzing these curves, the highest slope was observed for the enhanced surface produced by electromachining process for all tested mass flow rates. It confirms previous findings and confirm that the highest values of the heat transfer coefficient were achieved for this enhanced surface. It can be noticed that the highest difference T_M-T_f up to 100 K on curve plots is observed at the highest mass flow rate, Fig. 9c. At lower mass flow rates the difference were lower (up to 80 K), see Fig. 9a,b.

5 Conclusions

The present paper discusses the flow boiling heat transfer research conducted in an annular minigap 1 mm wide with HFE 649 as the working fluid. The studies were carried out for several values of mass flow rate and increasing heat flux supplied to the heated surface, in the entire boiling region. Five enhanced heated surfaces contacted fluid in the minigap, produced by: sanding, electromachining process (spark erosion), threading (two types) and cutting, were used in experiments.

The one-dimensional mathematical method was used to calculate the heat transfer coefficient at the metal pipe-fluid interface. In the this calculation method, the cylindrical wall was assumed to be a planar multilayer wall. The results were presented as a function of the heat transfer coefficient along the minigap length and as boiling curves, prepared for selected values of mass flow rate and five types of the enhanced heated surface and a smooth one.

Observations indicated that the heat transfer coefficient decreased with the distance from the gap inlet in the subcooled and saturated boiling region, separately. Under the saturated boiling, local heat transfer coefficients achieved higher values compared to those in the subcooled boiling region. The highest local values of heat transfer coefficient were obtained for enhanced surface produced by electromachining process at the saturated boiling region, for analyzed mass flow rates and similar heat fluxes. Local values of heat transfer coefficient received for 2nd type threaded surface were the lowest, even compared with data obtained for a smooth surface. The boiling curves generated for two distances from the minigap inlet have similar plots without wall temperature drop characteristic for nucleation hysteresis. The highest temperature difference up to 100 K on curve plots was observed at the highest mass flow rate.

References

1. G. Boye, J. Schmidt, F. Beyrau, Adv. Mech. Eng. **7**(6), 1–14 (2015)
2. C.P. Yin, Y.Y. Yan, T.F. Lin, B.C. Yang, Int. J. Heat Mass Transf. **43**, 1885–1896 (2000)
3. F.C. Hsieh, K.W. Li, Y.M. Lie, C.A. Chen, T.F. Lin, Int. J. Heat Mass Transfer **51**, 3763–3775 (2008)
4. C.A. Chen, W.R. Chang, K.W. Li, Y.M. Lie, T.F. Lin, Int. J. Heat Mass Transf. **52**, 3147–3158 (2009)
5. T. Musiał, M. Piasecka, S. Hożejowska, EPJ Web of Conf. **143**, 02077 (2017)
6. M. Piasecka, S. Hożejowska, T. Musiał, E3S Web of Conf. **13**, 02002 (2017)
7. M. Piasecka, S. Hożejowska, A. Piasecki, *Proc. 9th World Conf. ExHFT-9, 12-15.06.2017, Iguazu Falls, Brazil*, PT30 (2017)
8. S. Hożejowska, M. Piasecka, *Proc. ICCHMT 2018, 21-24.05.2018, Cracow, Poland* (2018) (to be published in MATEC Web of Conf.)
9. M. Piasecka, K. Strąk, B. Grabas, Arch. Metall. Mater. **62**(4), 1983–1990 (2017)
10. B. Maciejewska, M. Piasecka, Int. J. Heat Mass Transf. **107**, 925–933 (2017)
11. B. Maciejewska, M. Piasecka, Heat Mass Transf. **53**, 1211–1224 (2017)
12. B. Maciejewska, K. Strąk, M. Piasecka, Procedia Eng. **157**, 82–88 (2016)
13. K. Strąk, M. Piasecka, B. Maciejewska, Int. J. Heat Mass Transf. **117**, 375–387 (2018)
14. M. Piasecka, K. Strąk, Heat Transf. Eng. **40**(13-14) (2019) in print, DOI 10.1080/01457632.2018.1457264
15. B. Grabas, Exp. Therm. Fluid Sci. **68**, 499–508 (2015)
16. W. Depczyński, J. Achiev. Mater. Manuf. Eng. **66**(2), 67–72 (2014)
17. N. Radek, J. Konstanty, M. Scendo, Arch. Metall. Mater. **60**, 2579–2584 (2015)
18. R. Pastuszko, M. Piasecka, J. Physics Conf. **395**, 012137 (2012)
19. R. Kaniowski, R. Pastuszko, L. Nowakowski, EPJ Web of Conf. **143**, 02049 (2017)
20. R. Kaniowski, R. Pastuszko, EPJ Web of Conf. **143**, 02050 (2017)
21. R. Kaniowski, R. Pastuszko, EPJ Web of Conferences **180**, 02041 (2018)
22. R. Pastuszko, M.E. Poniewski, M. Koziol, Heat Mass Transf. **48** 1367–1374 (2012)
23. R. Pastuszko, R. Kaniowski, EPJ Web of Conf. **25**, 02019 (2012)
24. L. Dąbek, A. Kapjor, L. J. Orman, MATEC Web Conf. **168**, 07001 (2018)
25. L. J Orman, J Enhanced Heat Tran. **23**(2),137–153 (2016)
26. S. Błasiak, A. Zahorulko, Tribol. Int. **94**, 126–137 (2016)
27. S. Błasiak, Int. J. Heat Mass Transf. **100**, 78–88 (2016)
28. S. Błasiak, Int. J. Heat Mass Transf. **81**, 90–102 (2015)

29. M. Piasecka, Metrol. Meas. Syst. **XX**(2), 205–216 (2013)
30. M. Piasecka, Adv. Mater. Research **874**, 95–100 (2014)
31. M. Piasecka, Exp. Heat Tran. **27**, 231–255 (2014)